

AD-A250 487



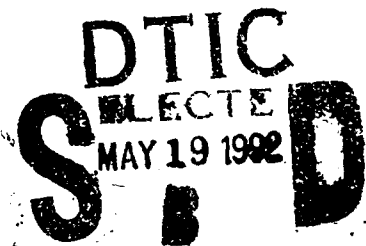
AD

TECHNICAL REPORT ARCCB-TR-92013

**A GENERALIZED PLANE-STRAIN
ELASTIC STRESS SOLUTION FOR A
MULTIORTHOTROPIC-LAYERED CYLINDER**

MARK D. WITHERELL

MARCH 1992



**US ARMY ARMAMENT RESEARCH,
DEVELOPMENT AND ENGINEERING CENTER
CLOSE COMBAT ARMAMENTS CENTER
BENÉT LABORATORIES
WATERVLIET, N.Y. 12189-4050**



APPROVED FOR PUBLIC RELEASE; DISTRIBUTION UNLIMITED

92-13278



DISCLAIMER

The findings in this report are not to be construed as an official Department of the Army position unless so designated by other authorized documents.

The use of trade name(s) and/or manufacturer(s) does not constitute an official indorsement or approval.

DESTRUCTION NOTICE

For classified documents, follow the procedures in DoD 5200.22-M, Industrial Security Manual, Section II-19 or DoD 5200.1-R, Information Security Program Regulation, Chapter IX.

For unclassified, limited documents, destroy by any method that will prevent disclosure of contents or reconstruction of the document.

For unclassified, unlimited documents, destroy when the report is no longer needed. Do not return it to the originator.

REPORT DOCUMENTATION PAGE

Form Approved
OMB No. 0704-0188

Public reporting burden for this collection of information is estimated to average 1 hour per response, including the time for reviewing instructions, searching existing data sources, gathering and maintaining the data needed, and completing and reviewing the collection of information. Send comments regarding this burden estimate or any other aspect of this collection of information, including suggestions for reducing this burden, to Washington Headquarters Services, Directorate for Information Operations and Reports, 1215 Jefferson Davis Highway, Suite 1204, Arlington, VA 22202-4302, and to the Office of Management and Budget, Paperwork Reduction Project (0704-0188), Washington, DC 20503.

1. AGENCY USE ONLY (Leave blank)		2. REPORT DATE March 1992	3. REPORT TYPE AND DATES COVERED Final	
4. TITLE AND SUBTITLE A GENERALIZED PLANE-STRAIN ELASTIC STRESS SOLUTION FOR A MULTIORTHOTROPIC-LAYERED CYLINDER			5. FUNDING NUMBERS AMCMS: 6126.23.1BL0.0 PRON: 1A72ZH3HNMSC	
6. AUTHOR(S) Mark D. Witherell				
7. PERFORMING ORGANIZATION NAME(S) AND ADDRESS(ES) U.S. Army ARDEC Benet Laboratories, SMCAR-CCB-TL Watervliet, NY 12189-4050			8. PERFORMING ORGANIZATION REPORT NUMBER ARCCB-TR-92013	
9. SPONSORING / MONITORING AGENCY NAME(S) AND ADDRESS(ES) U.S. Army ARDEC Close Combat Armaments Center Picatinny Arsenal, NJ 07806-5000			10. SPONSORING / MONITORING AGENCY REPORT NUMBER	
11. SUPPLEMENTARY NOTES To be presented at the Seventh International Conference on Pressure Vessel Technology, 31 May - 5 June 1992, Dusseldorf, Germany. To be published in Proceedings of the Conference.				
12a. DISTRIBUTION / AVAILABILITY STATEMENT Approved for public release; distribution unlimited.			12b. DISTRIBUTION CODE	
13. ABSTRACT (Maximum 200 words) A methodology is presented for constructing an exact stress solution for a multiorthotropic-layered cylinder for which all layers have equivalent axial strain. Combined loadings of internal pressure, external pressure, and axial force are included in the solution's formulation. The multilayered solution is developed by applying the proper boundary conditions to a three-dimensional elasticity solution for a monolayered orthotropic cylinder. Theoretical results for multilayered cylinders with selected material layups and loading conditions are compared with finite element results to verify the accuracy of the solu- tion's formulation. The software implementation of this solution provides the design engineer with a powerful tool for efficiently using composite materials in cylindrical pressure vessels.				
14. SUBJECT TERMS Composite, Multilayered, Cylinder, Stresses, Orthotropic			15. NUMBER OF PAGES 20	
			16. PRICE CODE	
17. SECURITY CLASSIFICATION OF REPORT UNCLASSIFIED	18. SECURITY CLASSIFICATION OF THIS PAGE UNCLASSIFIED	19. SECURITY CLASSIFICATION OF ABSTRACT UNCLASSIFIED	20. LIMITATION OF ABSTRACT UL	

TABLE OF CONTENTS

	<u>Page</u>
ABSTRACT	1
INTRODUCTION	1
GEOMETRY, MATERIAL, AND LOADING DEFINITION	2
STRESS EQUATIONS FOR A MONOLAYERED ORTHOTROPIC CYLINDER	3
STRESS SOLUTION FOR A MULTIORTHOTROPIC-LAYERED CYLINDER	5
SOLUTION VERIFICATION	11
DISCUSSION OF RESULTS	12
CONCLUSION	12
REFERENCES	12
APPENDIX	18

TABLES

1.	MATERIAL PROPERTIES FOR IM6/EPOXY 55% FIBER-VOLUME RATIO	13
2.	COMPARISON BETWEEN MULTILAYERED SOLUTION AND ABAQUS FINITE ELEMENT SOLUTION	14

LIST OF ILLUSTRATIONS

1.	Monolayered cylinder geometry and loading for SOL1 and SOL2	15
2.	Three solutions combine to form the generalized plane-strain multilayered solution	16
3.	Stress and strain versus radial position	17

Accession For NITS GRA&I DTIC TAB Unannounced Justification	<input checked="" type="checkbox"/> <input type="checkbox"/> <input type="checkbox"/>	By Distribution/	Availability Codes Avail and/or Special	2 A-1
---	---	---------------------	---	--------------

4

A Generalized Plane-Strain Elastic Stress Solution For A Multiorthotropic-Layered Cylinder

Mark D. Witherell

U.S. Army ARDEC, Close Combat Armaments Center, Benet Laboratories,
Watervliet, NY 12189-4050, USA

Abstract

A methodology is presented for constructing an exact stress solution for a multiorthotropic-layered cylinder for which all layers have equivalent axial strain. Combined loadings of internal pressure, external pressure, and axial force are included in the solution's formulation. The multilayered solution is developed by applying the proper boundary conditions to a three-dimensional elasticity solution for a monolayered orthotropic cylinder. Theoretical results for multilayered cylinders with selected material layups and loading conditions are compared with finite element results to verify the accuracy of the solution's formulation. The software implementation of this solution provides the design engineer with a powerful tool for efficiently using composite materials in cylindrical pressure vessels.

1. Introduction

Composite materials have become important in structural applications requiring high stiffness and low weight. This situation also exists in a current problem with Army cannon. The Army is interested in using composite materials to lengthen cannon while still maintaining the inertial characteristics of the shorter cannon. The design and analysis of these new cannon require a stress solution for thick-walled composite cylinders.

1.1 Monolayered Stress Solutions

The simplest type of cannon construction involves the use of only one material layer. The well-known stress solution by Lamé in 1852, as outlined in [1], is sufficient to characterize the state of stress for a monolayered isotropic cylinder. Lekhnitskii [2] developed a more general stress solution for a monolayered anisotropic cylinder. Recently, O'Hara [3] investigated Lekhnitskii's equations, simplifying them for the case of an orthotropic material under loadings of internal pressure, external pressure, and axial force. Shaffer [4] and Bieniek, Spillers, and Freudenthal [5] also investigated stress solutions for monolayered cylinders made from special types of orthotropic materials.

1.2 Multilayered Stress Solutions

In real applications, however, cylinders are often constructed from many composite layers where the fibers are wound or layed up at various angles. Most commonly, fibers are used in + and - wrap angle pairs, where each pair can be viewed as a single orthotropic layer. The whole structure can be considered a multiorthotropic-layered cylinder. Stress solutions for bilayered cylinders

have been investigated by Shaffer [6] and Witherell and Scavullo [7]. For multiorthotropic-layered cylinders, stress solutions have been developed by Bieniek, Spillers, and Freudenthal [5], Roy and Tsai [8], and Witherell [9]. The solution by Roy and Tsai is the most general and is a very good approximate stress solution for a multiorthotropic-layered cylinder with generalized plane-strain boundary conditions under loadings of internal and external pressure and axial force.

1.3 Exact Multilayered Stress Solution For Generalized Plane-Strain Boundary Conditions

This paper is similar to the work of Roy and Tsai [8], but whereas the development of their multilayered solution does not include the total contribution to the hoop strain equivalence condition from the radial and hoop stress produced by an axial force component, the solution discussed in this paper does. The inclusion of these two hoop strain contributions in the solution is not trivial, but it does result in a multilayered stress solution that is more rigorously correct than that of Roy and Tsai. For several material layups and loading conditions the author has investigated, the difference between the stress solution in this paper and that of Roy and Tsai is small (less than 10 percent). To some degree this small difference is to be expected, since the components neglected in the Roy-Tsai solution are of a secondary nature being a consequence of dissimilar Poisson contraction or expansion among axially loaded layers. However, there may be some material layups and loading conditions where this difference is greater. In addition, the exact solution presented in this paper provides a solid foundation for developing other stress solutions and eliminates any unnecessary uncertainties that would be associated with building on a less accurate approximate stress solution. For example, the solution that follows is a necessary part of the complete formulation for the exact thermal stress solution for a multilayered cylinder with generalized plane-strain boundary conditions. This paper describes the methodology of constructing the exact elastic stress solution for a multiorthotropic-layered cylinder under loadings of internal and external pressures and axial force. A comparison is then made between the exact multilayered solution and a finite element solution to verify the solution procedure.

2. Geometry, Material, and Loading Definition

A multilayered cylinder can be viewed as an assembly of many single-layered cylinders. It is fitting, therefore, to begin with a review of the monolayered orthotropic cylinder problem. There are actually two monolayered solutions that are used to construct the generalized plane-strain monolayered stress solution for internal and external pressures and axial force. The first solution, called SOL1, is for internal and external pressure loadings with plane-strain boundary conditions (zero axial strain). The second solution, called SOL2, is for axial loading with generalized plane-strain boundary conditions (constant axial strain).

2.1 Monolayered Problem

In the monolayered case, the cylinder is assumed to be long with ends that are either fixed, as in SOL1, or parallel such that the axial strain is uniform, as in SOL2. The geometry and loading for SOL1 and SOL2 are shown in Fig. 1. The

cylinder has an inner radius 'a' and an outer radius 'b'. For SOL1, the cylinder is subjected to internal pressure 'p' and external pressure 'q', and it has an axial force F_{z1} necessary to enforce the plane-strain axial constraint. For SOL2, the cylinder is only subjected to an axial force F_{z2} . For both SOL1 and SOL2, a cylindrically-orthotropic material is assumed with its principal axes coincident with the cylindrical coordinate system defining the cylinder geometry. An orthotropic material is characterized by nine independent material constants consisting of three engineering moduli (E_1, E_2, E_3), three shear moduli (G_{12}, G_{23}, G_{31}), and three Poisson's ratios ($\nu_{12}, \nu_{23}, \nu_{31}$). The numbers 1,2,3 indicate the principal material directions. For the above assumptions, the 1,2,3 directions correspond to the radial, hoop, and axial directions of the cylinder (r, θ, z). In addition, since the principal stress directions correspond to the principal directions of both the cylinder geometry and the applied loadings, shear effects are eliminated, and the number of material constants necessary for the analysis reduces to six.

3. Stress Equations For a Monolayered Orthotropic Cylinder

Lekhnitskii's two solutions for a cylinder with one anisotropic layer were simplified by O'Hara [3] for the case of a cylindrically-orthotropic material. The equations for these two solutions (SOL1 and SOL2) are given in the Appendix and are identical to those found in O'Hara's report with several corrections for some minor typographical errors. SOL1 and SOL2 each include three stress equations corresponding to the r , θ , and z directions. SOL1 also contains an equation which defines F_{z1} , the axial force necessary to enforce the plane-strain axial constraint. SOL2 also has an additional equation that contains a complicated constant (T) used in the three other stress equations.

3.1 Monolayered Stress Components at Inner and Outer Surfaces

In developing the multilayered solution, applying the correct boundary conditions at the interface of two orthotropic layers necessitates the use of stress values evaluated at the inner ($r=a$) and outer ($r=b$) surfaces of each layer. This evaluation process leads to six stress equations for SOL1 and six stress equations for SOL2 given below.

SOL1 - Stress equations evaluated at inner radius ($r = a$):

$$\sigma_{r,a} = RAP \cdot p + RAQ \cdot q \quad (1)$$

$$RAP = -1, \quad RAQ = 0$$

$$\sigma_{\theta,a} = TAP \cdot p + TAQ \cdot q \quad (2)$$

$$TAP = \frac{k(1+C_o^{2k})}{(1-C_o^{2k})}, \quad TAQ = \frac{-2kC_o^{k-1}}{(1-C_o^{2k})}$$

$$\sigma_{z,a} = ZAP \cdot p + ZAQ \cdot q \quad (3)$$

$$ZAP = \frac{(A_{13} - A_{23} \cdot TAP)}{A_{33}}, \quad ZAQ = \frac{-A_{23} \cdot TAQ}{A_{33}}$$

SOL1 - Stress equations evaluated at outer radius (r = b):

$$\sigma_{r,b} = RBP \cdot p + RBQ \cdot q \quad (4)$$

$$RBP = 0, \quad RBQ = -1$$

$$\sigma_{\theta,b} = TBP \cdot p + TBQ \cdot q \quad (5)$$

$$TBP = -TAQ \cdot C_0^2, \quad TBQ = -TAP$$

$$\sigma_{z,b} = ZBP \cdot p + ZBQ \cdot q \quad (6)$$

$$ZBP = -ZAQ \cdot C_0^2, \quad ZBQ = -ZAP + \frac{2A_{13}}{A_{33}}$$

The axial force equation for SOL1 can also be rewritten in a similiar form

$$F_{z1} = FZP \cdot p + FZQ \cdot q \quad (7)$$

$$FZP = \frac{2\pi a^2}{A_{33}} \left[\frac{[(TAP+TAQ+1)(A_{23}-A_{13})]}{(1-k^2)} - A_{23} \right]$$

$$FZQ = -\frac{2\pi b^2}{A_{33}} \left[\frac{[(TBP+TBQ+1)(A_{23}-A_{13})]}{(1-k^2)} - A_{23} \right]$$

where

$$C_0 = \frac{a}{b} \quad (8)$$

and the components A_{ij} are the elements of the compliance matrix for an orthotropic material, as given in the generalized Hooke's Law.

$$[\epsilon] = [A] [\sigma]$$

'k' is an orthotropic material constant given by

$$k = \sqrt{\frac{\beta_{11}}{\beta_{22}}} \quad (9)$$

where, in general,

$$\beta_{ij} = A_{ij} - \frac{A_{i3} A_{3j}}{A_{33}} \quad (10)$$

SOL2 - Stress equations evaluated at inner radius (r = a):

$$\sigma_{r,a} = 0 \quad (11)$$

$$\sigma_{\theta,a} = TAF \cdot F_{z2} \quad (12)$$

$$TAF = \frac{h}{T} (1+TAP+TAQ)$$

$$\sigma_{z,a} = ZAF \cdot F_{z2} \quad (13)$$

$$ZAF = \frac{1}{T} - \frac{A_{23} \cdot TAF}{A_{33}}$$

SOL2 - Stress equations evaluated at outer radius ($r = b$):

$$\sigma_{r,b} = 0 \quad (14)$$

$$\sigma_{\theta,b} = \text{TBF} \cdot F_{z2} \quad (15)$$

$$\text{TBF} = \frac{h}{\tau} (1 + \text{TBP} + \text{TBQ})$$

$$\sigma_{z,b} = \text{ZBF} \cdot F_{z2} \quad (16)$$

$$\text{ZBF} = \frac{1}{\tau} - \frac{A_{23} \cdot \text{TBF}}{A_{33}}$$

where

$$h = \frac{A_{23} - A_{13}}{\beta_{11} - \beta_{22}} \quad (17)$$

and

$$\begin{aligned} \tau = \pi(b^2 - a^2) - \frac{2\pi h}{A_{33}} & \left[\frac{b^2 - a^2}{2} (A_{13} + A_{23}) - \frac{b^2(1 - C_0^{k+1})^2}{(1 - C_0^{2k})} \frac{(A_{13} + kA_{23})}{(1+k)} \right. \\ & \left. + \frac{a^2(1 - C_0^{k-1})^2}{(1 - C_0^{2k})} \frac{(A_{13} - kA_{23})}{(1-k)} \right] \end{aligned} \quad (18)$$

In each of the twelve stress equations above, there are constants (two for SOL1 and one for SOL2), e.g., TAP and TAQ for the $\sigma_{\theta,a}$ stress of SOL1 and TBF for the $\sigma_{\theta,b}$ of SOL2, which determine the magnitude of the contribution to the given stress caused by either the internal or external pressure for SOL1 or the axial force for SOL2. These constants are material- and geometry-dependent, and each has a three-letter name. The first letter corresponds to the stress direction (r, θ, z), the second letter signifies the point at which the stress has been evaluated (a, b), and the third letter corresponds to either the pressure (q, p) it is applied to or the axial force F_{z2} . For example, TAQ is the constant for the θ stress, evaluated at $r = a$ (\underline{A}), magnifying the external pressure q (\underline{Q}), and ZBF is the constant for the z stress, evaluated at $r = b$ (\underline{B}), magnifying the axial force F_{z2} .

4. Stress Solution For a Multiorthotropic-Layered Cylinder

In this section we discuss the methodology of constructing the stress solution for a multilayered cylinder, where each layer has material and geometry definitions identical to those previously discussed for the monolayered case. The solutions SOL1 and SOL2 are used as the basis for the multilayered solution.

4.1 Decomposition of the Generalized Plane-Strain Multilayered Solution

The complete multilayered solution for internal pressure, external pressure, and axial force loadings with generalized plane-strain boundary conditions is constructed from the superposition of three separate multilayered solutions. Figure 2 shows the decomposition of the overall problem into its three parts. The first solution, called MSOL1, is the multilayered plane-strain solution for

internal and external pressure. This solution requires finding the set of interface pressures such that the hoop strain of each layer at every two-layer interface is equal. Stated another way, the radial displacement must be continuous through the cylinder (no gaps). This solution, which uses SOL1, has already been obtained by Withereff [9]. The total axial force necessary to enforce the plane-strain boundary conditions for MSOL1 is denoted as F_{z1t} and is the summation of the axial forces for each of the layers (F_{z1}) as given in Eq. (7). The second solution, called MSOL2 (or the axial force solution), is the multilayered solution obtained by applying an axial force to each layer such that all the layers have equivalent axial strain. For this solution, each layer is considered independent, and thus gaps or overlaps result at each layer interface once the axial forces are applied. These gaps or overlaps are taken care of in the third solution. It should be noted that the axial strain produced in each of these layers is the total axial strain for the overall solution. The total axial force that results for the MSOL2 solution is equal to the sum of the axial forces on each layer (F_{z2}) and is denoted as F_{z2t} . Finally, the third solution, called MSOL3, is a plane-strain solution for a set of interface pressures that eliminates the gaps or overlaps produced by MSOL2. MSOL3 is called the plane-strain equilibrating solution because it equilibrates the hoop strain at the layer interfaces by removing the gaps or overlaps produced by MSOL2. The form of the solution for MSOL3 is identical to MSOL1, except that it does not have internal or external pressures acting on the overall cylinder (this was accomplished in MSOL1), only pressures acting on the interfaces of each layer. Also, since MSOL3 is a plane-strain solution, it does not affect the total axial strain of the MSOL2 solution. The MSOL3 solution does, however, produce a total axial force which must be accounted for. The total axial force for MSOL3 is denoted as F_{z3t} and is obtained by the summation of all the layer axial forces (F_{z3}) (F_{z3} is of the same form as F_{z1} in Eq.(7)) produced by the interface pressures of MSOL3. The net axial force for the overall solution, prescribed for a given problem, is denoted as F_{net} and is equal to the sum of F_{z1t} , F_{z2t} , and F_{z3t} . The following section contains the necessary details for constructing the MSOL1, MSOL2, and MSOL3, as well as combining these three solutions to obtain the overall solution.

4.2 The MSOL1 Multilayered Solution

MSOL1 is the solution for the multilayered cylinder with internal and external pressure under plane-strain boundary conditions and, as mentioned earlier, has already been developed. The following discussion gives the important aspects of this solution also used to develop MSOL3.

4.2.1 Step 1 For MSOL1

The first step in constructing MSOL1 is to equate the circumferential (hoop) strain of adjacent orthotropic layers at their interface. In other words, we equate the hoop strain at $r = b$ of the i th layer with the hoop strain at $r = a$ of the $i+1$ layer

$$\epsilon_{\theta,b(i)} = \epsilon_{\theta,a(i+1)} \quad (19)$$

Recalling that $[\epsilon] = [A][\sigma]$, 1,2,3 correspond to the r,θ,z directions, and by using the stress equations of SOL1 with $q(i-1) = p(i)$, we have

$$G_{i1} \cdot q(i-1) + G_{i2} \cdot q(i) + G_{i3} \cdot q(i+1) = 0 \quad (20)$$

where

$$G_{i1} = -C_0^2(i) \cdot \beta_{22}(i) \cdot TAQ(i)$$

$$G_{i2} = -[\beta_{12}(i) - \beta_{12}(i+1) + \beta_{22}(i) \cdot TAP(i) + \beta_{22}(i+1) \cdot TAP(i+1)]$$

$$G_{i3} = -\beta_{22}(i+1) \cdot TAQ(i+1)$$

4.2.2 System of Equations For MSOL1

For each two-layer combination there is one equation defining the hoop strain equivalence condition. For a cylinder with 'N' orthotropic layers, there are N-1 equations and N-1 unknowns. Setting up these equations in matrix form and noting that p(1) and q(N) are the prescribed internal and external pressures of the overall cylinder results in

$$\begin{bmatrix} G_{12} & G_{13} & & & & \\ G_{21} & G_{22} & G_{23} & & & 0 \\ & G_{31} & G_{32} & G_{33} & & \\ & & - & - & - & \\ & & & - & - & - \\ & & & & \cdot & \\ & 0 & & & \cdot & \\ & & G_{N-2,1} & G_{N-2,2} & G_{N-2,3} & \\ & & & G_{N-1,1} & G_{N-1,2} & \end{bmatrix} \begin{bmatrix} q(1) \\ q(2) \\ q(3) \\ \cdot \\ \cdot \\ \cdot \\ \cdot \\ q(N-1) \end{bmatrix} = \begin{bmatrix} -G_{11} \cdot p(1) \\ 0 \\ 0 \\ \cdot \\ \cdot \\ \cdot \\ \cdot \\ -G_{N-1,3} \cdot q(N) \end{bmatrix} \quad (21)$$

or

$$[G] [Q] = [R] \quad (22)$$

4.2.3 Stress Distribution in Each Layer For MSOL1

This system of equations can be easily solved to determine the interface pressure vector [Q]. By recalling that $q(i-1) = p(i)$, we can now calculate the stress distribution in layer i using the general stress equations for SOL1 found in the Appendix with p(i) and q(i) as input.

4.2.4 Total Axial Force For MSOL1

In addition to finding the stress distribution in layer i, the axial force necessary to constrain layer i to zero axial strain can be calculated using Eq. (7) with p(i) and q(i) as input. By summing the axial forces on each layer, we can determine the total axial force, F_{z1t} , for MSOL1

$$F_{z1t} = \sum_{i=1}^N F_{z1}(i) \quad (23)$$

4.3 The MSOL2 and MSOL3 Multilayered Solutions

Next, we proceed with the MSOL2 and MSOL3 solutions, which need to be looked at together. Since the internal and external pressure loadings were already taken care of in MSOL1, they are not included here. However, we need to bring the the total axial force F_{z1t} of MSOL1 into this discussion because it is part of the net axial force on the cylinder.

4.3.1 Step 1: Equating the Axial Strain of Each Layer (Each Layer Independent)

We accomplish this by equating the axial strain at the external surface of each layer ($r=b$) to that of layer 1

$$\epsilon_{z,b}(1) = \epsilon_{z,b}(i) \quad (24)$$

By substituting Hooke's Law with the stress components from SOL2, we arrive at an expression for the axial force of layer i in terms of the axial force of layer 1 and the material and geometry properties of layer 1 and layer i

$$F_{z2}(i) = F_{z2}(1) \frac{CAX(1)}{CAX(i)} \quad (25)$$

where

$$CAX(i) = A_{32}(i) \cdot TBF(i) + A_{33}(i) \cdot ZBF(i) \quad (26)$$

4.3.2 Step 2: Equating the Hoop Strain at Each Layer Interface

This step requires consideration of only MSOL2 and MSOL3 solutions, since the hoop strain equivalence at each layer interface was already satisfied in MSOL1

$$\epsilon_{\theta,b}(i) = \epsilon_{\theta,a}(i+1) \quad (19)$$

The hoop strain at the interface of layer i and $i+1$ has contributions from the two stress solutions MSOL2 and MSOL3:

$$\epsilon_{\theta,b}(i) + \epsilon_{\theta,b}(i) = \epsilon_{\theta,a}(i+1) + \epsilon_{\theta,a}(i+1) \quad (27)$$

Axial Force
MSOL2

Plane-Strain Equilibrating
MSOL3

4.3.2.1 Axial Force Contribution to $\epsilon_{\theta,b}(i)$ and $\epsilon_{\theta,a}(i+1)$

Using Hooke's Law and the SOL2 solution gives

$$\epsilon_{\theta,b}(i) = F_{z2}(i) \cdot CTB(i) \quad (28)$$

where

$$CTB(i) = A_{22}(i) \cdot TBF(i) + A_{23}(i) \cdot ZBF(i) \quad (29)$$

Similarly,

$$\epsilon_{\theta,a}(i+1) = F_{z2}(i+1) \cdot CTA(i+1) \quad (30)$$

where

$$CTA(i+1) = A_{22}(i+1) \cdot TAF(i+1) + A_{23}(i+1) \cdot ZAF(i+1) \quad (31)$$

4.3.2.2 Plane-Strain Equilibrating Contribution to $\epsilon_{\theta,b}(i)$ and $\epsilon_{\theta,a}(i+1)$

From an earlier derivation of the plane-strain solution MSOL1

$$\epsilon_{\theta,b}(i) = \epsilon_{\theta,a}(i+1) \quad (19)$$

reduces to

$$G_{i1} \cdot q(i-1) + G_{i2} \cdot q(i) + G_{i3} \cdot q(i+1) = 0 \quad (20)$$

4.3.2.3 Combining the Axial Force and Plane-Strain Equilibrating Contributions Into Eq. (27)

$$F_{z2}(i) \cdot CTB(i) - F_{z2}(i+1) \cdot CTA(i+1) + G_{i1} \cdot q(i-1) + G_{i2} \cdot q(i) + G_{i3} \cdot q(i+1) = 0 \quad (32)$$

Now substituting Eq. (25) for $F_{z2}(i)$ and $F_{z2}(i+1)$ results in

$$F_{z2}(1) \cdot CAX(1) \left[\frac{CTB(i)}{CAX(i)} - \frac{CTA(i+1)}{CAX(i+1)} \right] + G_{i1} \cdot q(i-1) + G_{i2} \cdot q(i) + G_{i3} \cdot q(i+1) = 0 \quad (33)$$

At this point, the only unknowns are the axial force $F_{z2}(1)$ and the interface pressures $q(i-1)$, $q(i)$, and $q(i+1)$. Step 3 enables us to get $F_{z2}(1)$ in terms of the interface pressures and other known quantities, and thus we can solve the entire system of equations.

4.3.3 Step 3: Summation of Axial Forces

This step considers the total axial force contributions from MSOL1, MSOL2, and MSOL3

$$F_{net} = F_{z1t} + F_{z2t} + F_{z3t} \quad (34)$$

Both F_{net} and F_{z1t} are known values (F_{z1t} was calculated in MSOL1)

$$F_{z2t} = \sum_{i=1}^N F_{z2}(i) = F_{z2}(1) \cdot CAX(1) \cdot \left(\sum_{i=1}^N \frac{1}{CAX(i)} \right) \quad (35)$$

Also

$$F_{z3t} = \sum_{i=1}^N F_{z3}(i) = \sum_{i=1}^N (FZP(i) \cdot p(i) + FZQ(i) \cdot q(i)) \quad (36)$$

For the equilibrating solution, $p(1)$ and $q(N) = 0$ and $p(i+1) = q(i)$

$$F_{z3t} = \sum_{i=1}^{N-1} (FZP(i+1) + FZQ(i)) \cdot q(i) \quad (37)$$

$$F_{net} = F_{z1t} + F_{z2(1)} \cdot CAX(1) \cdot \left(\sum_{i=1}^N \frac{1}{CAX(i)} \right) + \sum_{i=1}^{N-1} \left[(FZP(i+1) + FZQ(i)) \cdot q(i) \right] \quad (38)$$

Solving for $F_{z2(1)}$ gives

$$F_{z2(1)} = \frac{F_{net} - F_{z1t} - \sum_{i=1}^{N-1} \left[(FZP(i+1) + FZQ(i)) \cdot q(i) \right]}{CAX(1) \cdot \left(\sum_{i=1}^N \frac{1}{CAX(i)} \right)} \quad (39)$$

Now, back substituting $F_{z2(1)}$ into the hoop strain equivalence condition for interface (i) gives

$$CEQ(i) \left[-F_{net} + F_{z1t} + \sum_{j=1}^{N-1} \left[(FZP(j+1) + FZQ(j)) \cdot q(j) \right] \right] + G_{i1} \cdot q(i-1) + G_{i2} \cdot q(i) + G_{i3} \cdot q(i+1) = 0 \quad (40)$$

where $CEQ(i)$ is given by

$$CEQ(i) = \frac{- \left[\frac{CTB(i)}{CAX(i)} - \frac{CTA(i+1)}{CAX(i+1)} \right]}{\left(\sum_{j=1}^N \frac{1}{CAX(j)} \right)} \quad (41)$$

4.3.4 Step 4: Solution Assembly

In matrix form, the set of $N-1$ hoop strain equivalence equations is given by

$$([F] + [G]) [QQ] = FZN \cdot [C] \quad (42)$$

where the components of $[F]$ are given by

$$F_{ij} = CEQ(i) \cdot (FZP(j+1) + FZQ(j)) \quad , \quad (1 \leq i, j \leq N-1) \quad (43)$$

and the components of the matrix $[G]$ and the vector $[QQ]$ are the same, as given by $[G]$ and $[Q]$ in Eqs. (21) and (22). The constant FZN is given by

$$FZN = F_{net} - F_{z1t} \quad (44)$$

and the components of the vector $[C]$ are given by

$$C_i = CEQ(i) \quad , \quad (1 \leq i \leq N-1) \quad (45)$$

The above matrix equation can be easily solved to determine the components of the vector $[QQ]$, the interface pressures.

4.4 Stress Distribution in Each Layer For the Generalized Plane-Strain Multilayered Stress Solution

In order to obtain the stress distribution in layer i for the generalized plane-strain multilayered solution, the following procedure must be employed:

1. The total interface pressure vector $[QT]$ must be obtained by adding $[Q]$ found from Eq. (22) with $[QQ]$ found from Eq. (42)

$$[QT] = [Q] + [QQ] \quad (46)$$

2. The axial force components $F_{z2}(i)$ must be obtained by

- calculating $F_{z2}(1)$ (Eq. (39)) using the components of $[QQ]$ for $q(i)$ and using F_{z1t} obtained using $[Q]$ from MSOL1 in connection with Eqs. (7) and (23);
- using $F_{z2}(1)$ and Eq. (25), the $F_{z2}(i)$ components can now be obtained directly.

The stress distribution in layer i may now be obtained by superimposing the SOL1 solution using the components of $[QT]$ as input for $q(i)$ and $p(i)$ with the SOL2 solution, using $F_{z2}(i)$ as input for F_{z2} .

5. Solution Verification

The exact multilayered solution was used to investigate the stress and strain distribution within a ten-layered cylinder ($N=10$). The cylinder had an inside radius $a(1) = 1$ inch, an outside radius $b(10) = 2$ inches, and each of the ten layers was 0.1 inch thick. The material used was an IM6/epoxy with a 55 percent fiber-volume ratio. The layup considered consisted of five hoop-axial pairs starting at the inside radius of the cylinder. The material properties for the hoop and axial fiber orientations are given in Table 1. The loading conditions for the case considered included internal pressure ($p(1) = 2$ psi), external pressure ($q(10) = 1$ psi), and axial force ($F_{net} = 10$ lbs). The results for this case are shown in the four plots of Fig. 3. The plots show the r, θ, z stress and strain distributions as a function of radial position in the cylinder.

5.1 Finite Element Solution Used in Comparison

The multilayered solution for the above-mentioned case was also compared to a finite element solution for the same case. The ABAQUS finite element code was used to produce the stress results used in the comparison. The finite element model contained 20 eight-node quadratic axisymmetric elements with two equal-sized elements used to model each of the ten orthotropic layers. The comparison was limited to the radial, hoop, and axial stress values evaluated at the inner and outer radii of each orthotropic layer. Table 2 contains the results of this comparison.

6. Discussion of Results

6.1 Comparison of Exact Solution With Finite Element Solution

A comparison of the theoretical solution with the finite element solution for the radial, hoop, and axial stresses at the inner and outer surfaces of each orthotropic layer is shown in Table 1. For all three stress components, the comparison shows excellent agreement between the results generated by the theory and those from the finite element solution. For the finite element solution, the stresses were obtained at the nodes and were somewhat less accurate than the stresses obtained at the integration points of the element. This error, although very small, is seen most clearly by the fact that the radial stress value at the inner surface of the overall cylinder is not equal to the prescribed value of -2 psi.

6.2 Stress and Strain Distributions Produced by Exact Solution

In Fig. 3, the stress and strain distributions are displayed for the multi-layered cylinder with the same geometry and loading conditions as the case already discussed. As can be seen in the plot containing the radial and axial stress, the radial stress varies continuously from -2 psi at the inside radius to -1 psi at the outside radius. As is also seen in the plots, the axial layers take up the majority of the axial load, and the hoop layers sustain the highest levels of hoop stress. If the axial stress was integrated over the end surface area, it would be equal to the net axial force prescribed for the cylinder ($F_{net}=10$ lbs). The strain plots show the expected smooth and continuous curve for the hoop strain and the uniform axial strain, which the generalized plane-strain boundary conditions require.

7. Conclusion

An exact generalized plane-strain elastic stress solution for a multiorthotropic-layered cylinder has been developed for loadings of internal pressure, external pressure, and axial force. The software implementation of this stress solution has been shown to be in excellent agreement with finite element results.

References

1. Timoshenko, S.P., Goodier, J.N.: Theory of Elasticity; 3rd Edition, McGraw-Hill, New York, 1970 pp68-71.
2. Lekhnitskii, S.G.: Theory of Elasticity of an Anisotropic Elastic Body; Holden-Day Inc., San Francisco, 1963 pp243-257, (English translation of 1950 Russian edition).
3. O'Hara, G.P.: Some Results on Orthotropic High Pressure Cylinders; ARCCB-TR-87015, Benet Weapons Laboratory, Watervliet, NY, June 1987.
4. Shaffer, B.W.: Generalized Plane-Strain of Pressurized Orthotropic Tubes; Trans. of ASME, Series B, August 1965 pp337-343.

5. Bieniek, M., Spillers, W.R., Freudenthal, A.M.: Nonhomogeneous Thick-Walled Cylinder Under Internal Pressure; American Rocket Society Journal, Vol. 32, 1962 pp1249-1255.
6. Shaffer, B.W.: Pressurization of Two-Layered Incompressible Orthotropic Tubes; Journal of the Franklin Institute, Vol. 285, 1968 pp187-203.
7. Witherell, M.D., Scavullo, M.A.: Stress Analysis and Weight Savings of Internally Pressurized Composite-Jacketed Isotropic Cylinders; Journal of Pressure Vessel Technology, Vol. 112, No. 4, 1990 pp397-403.
8. Tsai, S.W.: Composites Design; 3rd Edition, Think Composites, Dayton, OH, 1987 pp23-1 - 23-21.
9. Witherell, M.D.: A Plane-Strain Elastic Stress Solution for a Multiorthotropic-Layered Cylinder; ARCCB-TR-90016, Benet Laboratories, Watervliet, NY, June 1990.

Table 1. Material Properties For IM6/Epoxy 55% Fiber-Volume Ratio

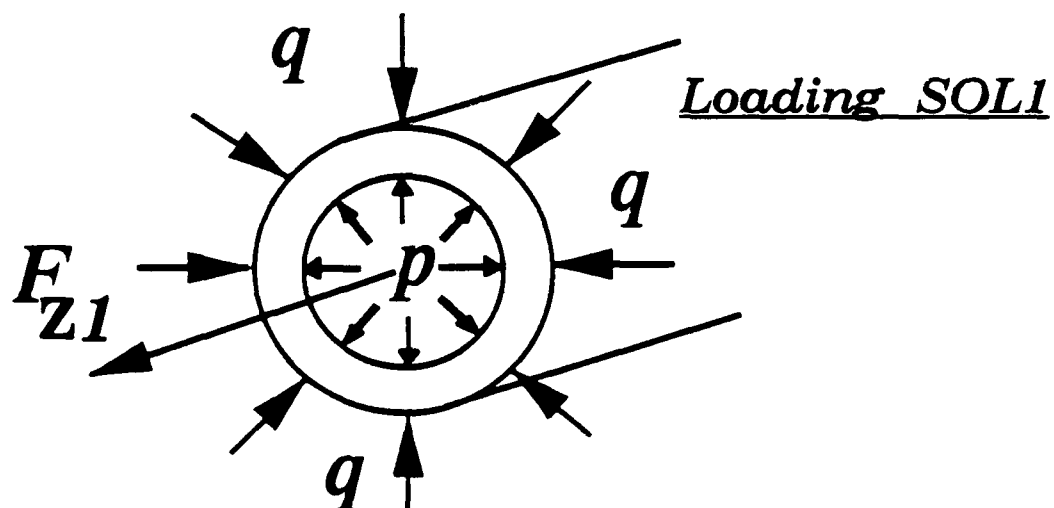
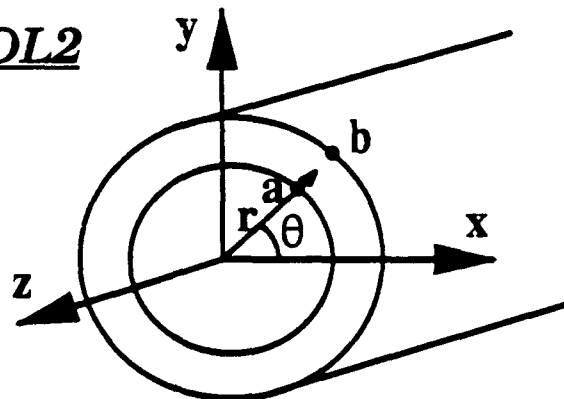
Fiber Direction	E_r (Mpsi)	E_θ (Mpsi)	E_z (Mpsi)	$\nu_{r\theta}$	$\nu_{\theta z}$	ν_{zr}
Hoop	1.126	23.31	1.126	0.0152	0.3147	0.3991
Axial	1.126	1.126	23.31	0.3991	0.0152	0.3147

Table 2. Comparison Between Multilayered Solution and ABAQUS Finite Element Solution
Generalized Plane-Strain Boundary Conditions
Using 20 CAX8 Elements

Number of Layers $N = 10$, $5 \times (1\text{-hoop}, 1\text{-axial})$, (see Table 1)
 $a(1) = 1 \text{ in.}$, $b(10) = 2 \text{ in.}$, $p(1) = 2 \text{ psi}$, $q(10) = 1 \text{ psi}$, $F_{\text{net}} = 10 \text{ lbs}$

Layer	Fiber Orient	Radius (in.)	Radial Stress (psi)		Hoop Stress (psi)		Axial Stress (psi)	
			Theory	ABAQUS	Theory	ABAQUS	Theory	ABAQUS
1	Hoop	1.0	-2.000	-1.987	8.557	8.564	-0.537	-0.531
		1.1	-1.208	-1.199	5.196	5.201	-0.271	-0.268
2	Axial	1.1	-1.208	-1.207	-0.174	-0.174	2.291	2.291
		1.2	-1.125	-1.124	-0.257	-0.256	2.291	2.292
3	Hoop	1.2	-1.125	-1.121	2.828	2.831	-0.275	-0.273
		1.3	-0.888	-0.884	1.195	1.196	-0.205	-0.203
4	Axial	1.3	-0.888	-0.887	-0.244	-0.244	2.369	2.369
		1.4	-0.843	-0.843	-0.288	-0.288	2.369	2.371
5	Hoop	1.4	-0.843	-0.842	-0.077	-0.076	-0.206	-0.206
		1.5	-0.828	-0.826	-1.108	-1.108	-0.216	-0.215
6	Axial	1.5	-0.828	-0.827	-0.332	-0.332	2.361	2.360
		1.6	-0.798	-0.797	-0.362	-0.362	2.361	2.362
7	Hoop	1.6	-0.798	-0.797	-1.969	-1.969	-0.217	-0.216
		1.7	-0.890	-0.890	-2.780	-2.780	-0.266	-0.266
8	Axial	1.7	-0.890	-0.890	-0.437	-0.437	2.308	2.308
		1.8	-0.866	-0.866	-0.461	-0.461	2.308	2.308
9	Hoop	1.8	-0.866	-0.865	-3.482	-3.482	-0.267	-0.267
		1.9	-1.023	-1.022	-4.221	-4.222	-0.341	-0.341
10	Axial	1.9	-1.023	-1.023	-0.557	-0.558	2.228	2.229
		2.0	-1.000	-1.000	-0.580	-0.580	2.228	2.229

Geometry
SOL1 & SOL2



Loading SOL2

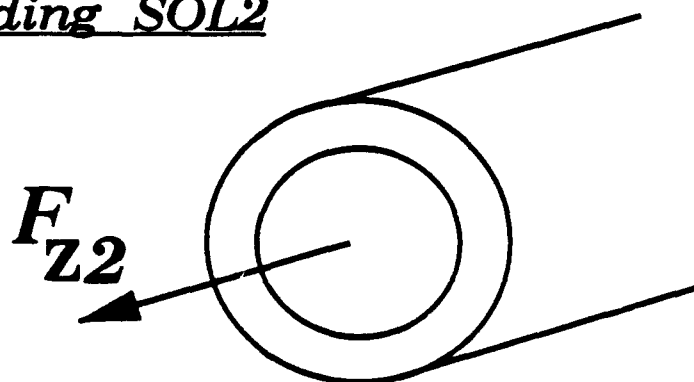
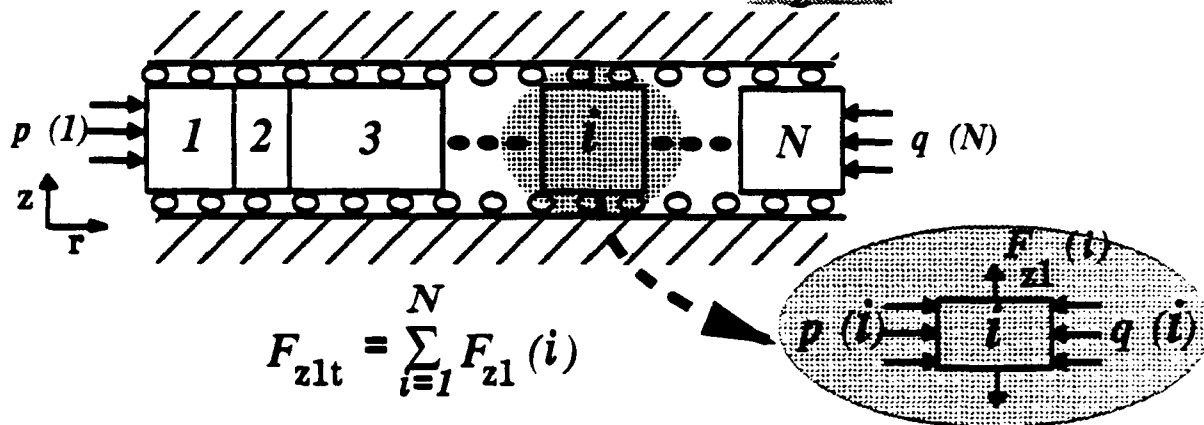
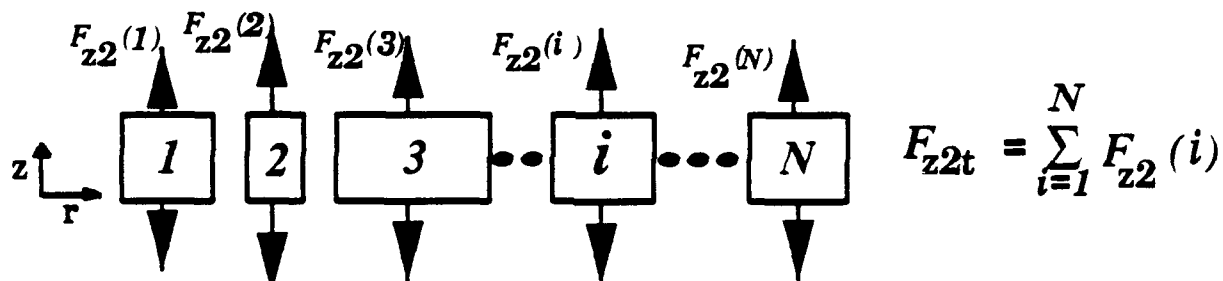


Fig. 1 Monolayered cylinder geometry and loading for SOL1 and SOL2.

1. MSOL1 - Plane Strain Solution $\epsilon_z = 0$



2. MSOL2 - Axial Force Solution $\epsilon_z \neq 0, \epsilon_z(i) = \epsilon_z(I)$



3. MSOL3 - Plane Strain Equilibrating Solution $\epsilon_z = 0$

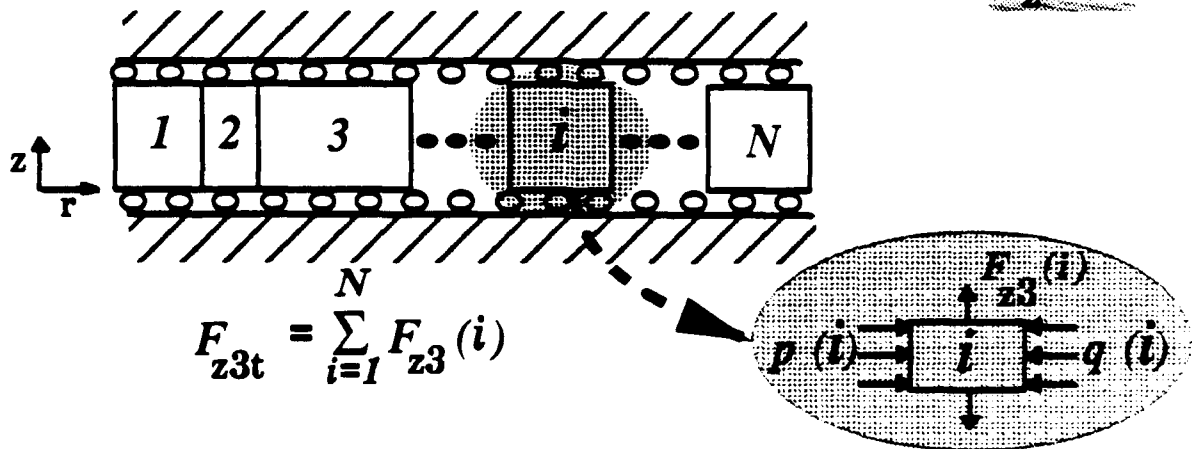


Fig. 2 Three solutions combine to form the generalized plane-strain multilayered solution.

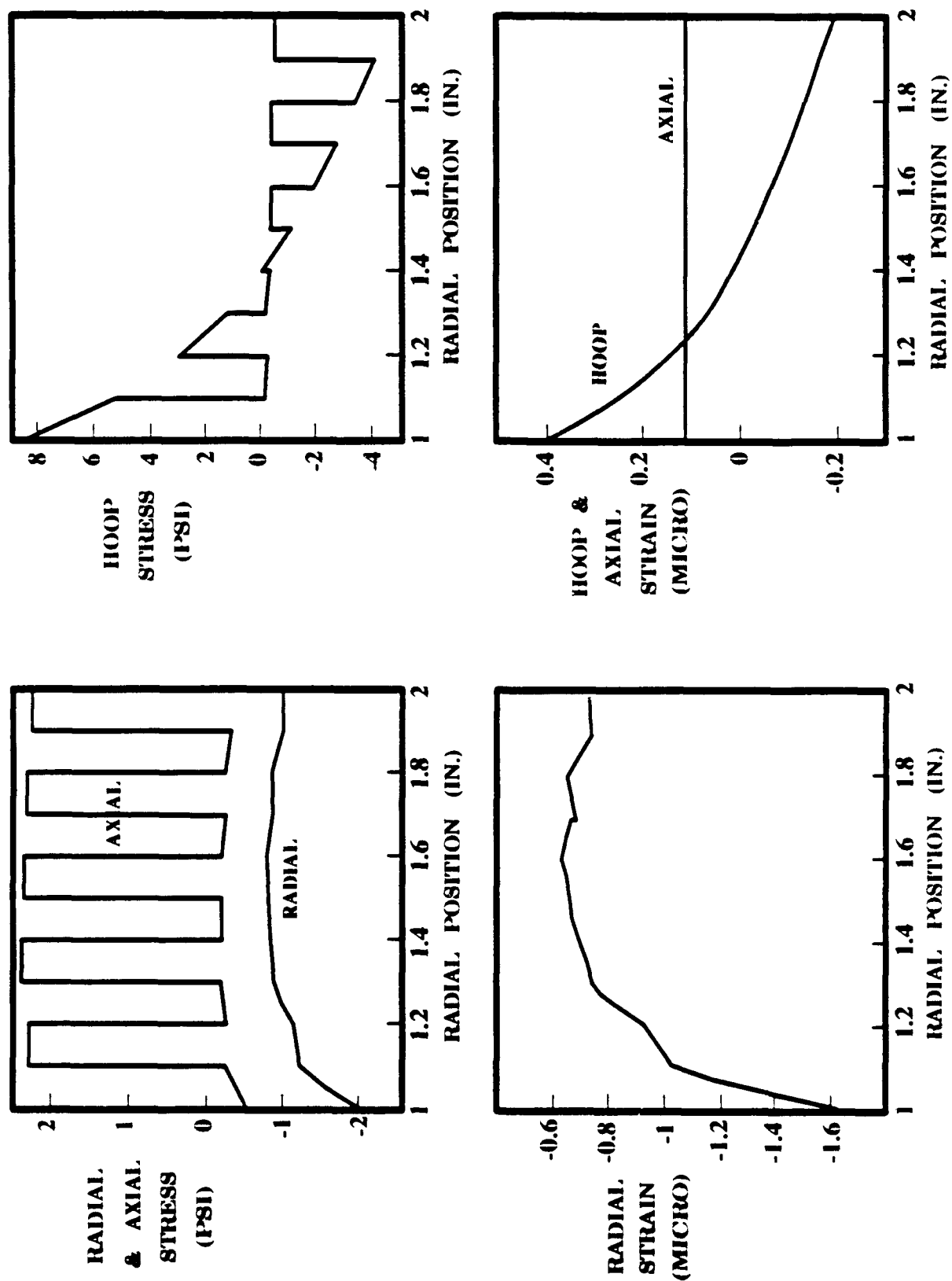


Fig. 3 Stress and strain versus radial position.

Appendix

SOL1 - Plane-Strain Solution For a Monolayered Orthotropic Cylinder Under Internal Pressure p and External Pressure q

$$\sigma_r = \left[\frac{pC_o^{k+1} - q}{(1-C_o^{2k})} \right] \left(\frac{r}{b} \right)^{k-1} + \left[\frac{qC_o^{k-1} - p}{(1-C_o^{2k})} \right] C_o^{k+1} \left(\frac{b}{r} \right)^{k+1}$$

$$\sigma_\theta = \left[\frac{pC_o^{k+1} - q}{(1-C_o^{2k})} \right] k \left(\frac{r}{b} \right)^{k-1} - \left[\frac{qC_o^{k-1} - p}{(1-C_o^{2k})} \right] k C_o^{k+1} \left(\frac{b}{r} \right)^{k+1}$$

$$\sigma_z = \frac{-1}{A_{33}} \left\{ \left[\frac{pC_o^{k+1} - q}{(1-C_o^{2k})} \right] (A_{13} + kA_{23}) \left(\frac{r}{b} \right)^{k-1} + \left[\frac{qC_o^{k-1} - p}{(1-C_o^{2k})} \right] (A_{13} - kA_{23}) C_o^{k+1} \left(\frac{b}{r} \right)^{k+1} \right\}$$

$$F_{z1} = \frac{2\pi}{A_{33}(1-C_o^{2k})} \left[b^2 (q - pC_o^{k+1}) (1-C_o^{k+1}) \frac{A_{13} + kA_{23}}{1+k} + a^2 (qC_o^{k-1} - p) (1-C_o^{k-1}) \frac{A_{13} - kA_{23}}{1-k} \right]$$

where ' r ' is the radial position in the cylinder.

SOL2 - Generalized Plane-Strain Solution For a Monolayered Orthotropic Cylinder Under Axial Force F_{z2}

$$\sigma_r = \frac{F_{z2} \cdot h}{T} \left[1 - \frac{(1-C_o^{k+1})}{(1-C_o^{2k})} \left(\frac{r}{b} \right)^{k-1} - \frac{(1-C_o^{k-1})}{(1-C_o^{2k})} C_o^{k+1} \left(\frac{b}{r} \right)^{k+1} \right]$$

$$\sigma_{\theta} = \frac{F_{z2} \cdot h}{T} \left[1 - \frac{(1-C_o^{k+1})}{(1-C_o^{2k})} k \left(\frac{r}{b}\right)^{k-1} + \frac{(1-C_o^{k-1})}{(1-C_o^{2k})} k C_o^{k+1} \left(\frac{b}{r}\right)^{k+1} \right]$$

$$\sigma_z = \frac{F_{z2}}{T} \left(1 - \frac{h}{A_{33}} \right) \left[A_{13} + A_{23} - \left[\frac{1 - C_o^{k+1}}{(1 - C_o^{2k})} (A_{13} + k A_{23}) \left(\frac{r}{b}\right)^{k-1} \right. \right. \\ \left. \left. - \left[\frac{(1-C_o^{k-1})}{(1-C_o^{2k})} (A_{13} - k A_{23}) C_o^{k+1} \left(\frac{b}{r}\right)^{k+1} \right] \right] \right]$$

TECHNICAL REPORT INTERNAL DISTRIBUTION LIST

	NO. OF COPIES
CHIEF, DEVELOPMENT ENGINEERING DIVISION	
ATTN: SMCAR-CCB-DA	1
-DC	1
-DI	1
-DR	1
-DS (SYSTEMS)	1
CHIEF, ENGINEERING SUPPORT DIVISION	
ATTN: SMCAR-CCB-S	1
-SD	1
-SE	1
CHIEF, RESEARCH DIVISION	
ATTN: SMCAR-CCB-R	2
-RA	1
-RE	1
-RM	1
-RP	1
-RT	1
TECHNICAL LIBRARY	5
ATTN: SMCAR-CCB-TL	
TECHNICAL PUBLICATIONS & EDITING SECTION	3
ATTN: SMCAR-CCB-TL	
OPERATIONS DIRECTORATE	1
ATTN: SMCWV-ODP-P	
DIRECTOR, PROCUREMENT DIRECTORATE	1
ATTN: SMCWV-PP	
DIRECTOR, PRODUCT ASSURANCE DIRECTORATE	1
ATTN: SMCWV-QA	

NOTE: PLEASE NOTIFY DIRECTOR, BENET LABORATORIES, ATTN: SMCAR-CCB-TL, OF ANY ADDRESS CHANGES.

TECHNICAL REPORT EXTERNAL DISTRIBUTION LIST

	<u>NO. OF COPIES</u>		<u>NO. OF COPIES</u>
ASST SEC OF THE ARMY RESEARCH AND DEVELOPMENT ATTN: DEPT FOR SCI AND TECH THE PENTAGON WASHINGTON, D.C. 20310-0103	1	COMMANDER ROCK ISLAND ARSENAL ATTN: SMCRI-ENM ROCK ISLAND, IL 61299-5000	1
ADMINISTRATOR DEFENSE TECHNICAL INFO CENTER ATTN: DTIC-FDAC CAMERON STATION ALEXANDRIA, VA 22304-6145	12	DIRECTOR US ARMY INDUSTRIAL BASE ENGR ACTV ATTN: AMXIB-P ROCK ISLAND, IL 61299-7260	1
COMMANDER US ARMY ARDEC ATTN: SMCAR-AEE	1	COMMANDER US ARMY TANK-AUTMV R&D COMMAND ATTN: AMSTA-DDL (TECH LIB) WARREN, MI 48397-5000	1
SMCAR-AES, BLDG. 321	1	COMMANDER US MILITARY ACADEMY	1
SMCAR-AET-O, BLDG. 351N	1	ATTN: DEPARTMENT OF MECHANICS WEST POINT, NY 10996-1792	
SMCAR-CC	1		
SMCAR-CCP-A	1	US ARMY MISSILE COMMAND REDSTONE SCIENTIFIC INFO CTR	2
SMCAR-FSA	1	ATTN: DOCUMENTS SECT, BLDG. 4484 REDSTONE ARSENAL, AL 35898-5241	
SMCAR-FSM-E	1		
SMCAR-FSS-D, BLDG. 94	1		
SMCAR-IMI-I (STINFO) BLDG. 59	2		
PICATINNY ARSENAL, NJ 07806-5000			
DIRECTOR US ARMY BALLISTIC RESEARCH LABORATORY ATTN: SLCBR-DD-T, BLDG. 305	1	COMMANDER US ARMY FGN SCIENCE AND TECH CTR ATTN: DRXST-SD 220 7TH STREET, N.E. CHARLOTTESVILLE, VA 22901	1
ABERDEEN PROVING GROUND, MD 21005-5066			
DIRECTOR US ARMY MATERIEL SYSTEMS ANALYSIS ACTV ATTN: AMXSY-MP	1	COMMANDER US ARMY LABCOM MATERIALS TECHNOLOGY LAB ATTN: SLCMT-IML (TECH LIB)	2
ABERDEEN PROVING GROUND, MD 21005-5071		WATERTOWN, MA 02172-0001	
COMMANDER HQ, AMCCOM ATTN: AMSMC-IMP-L	1		
ROCK ISLAND, IL 61299-6000			

NOTE: PLEASE NOTIFY COMMANDER, ARMAMENT RESEARCH, DEVELOPMENT, AND ENGINEERING CENTER, US ARMY AMCCOM, ATTN: BENET LABORATORIES, SMCAR-CCB-TL, WATERVLIET, NY 12189-4050, OF ANY ADDRESS CHANGES.

TECHNICAL REPORT EXTERNAL DISTRIBUTION LIST (CONT'D)

	<u>NO. OF COPIES</u>		<u>NO. OF COPIES</u>
COMMANDER US ARMY LABCOM, ISA ATTN: SLCIS-IM-TL 2800 POWDER MILL ROAD ADELPHI, MD 20783-1145	1	COMMANDER AIR FORCE ARMAMENT LABORATORY ATTN: AFATL/MN EGLIN AFB, FL 32542-5434	1
COMMANDER US ARMY RESEARCH OFFICE ATTN: CHIEF, IPO P.O. BOX 12211 RESEARCH TRIANGLE PARK, NC 27709-2211	1	COMMANDER AIR FORCE ARMAMENT LABORATORY ATTN: AFATL/MNF EGLIN AFB, FL 32542-5434	1
DIRECTOR US NAVAL RESEARCH LAB ATTN: MATERIALS SCI & TECH DIVISION CODE 26-27 (DOC LIB) WASHINGTON, D.C. 20375	1 1	MIAC/CINDAS PURDUE UNIVERSITY 2595 YEAGER ROAD WEST LAFAYETTE, IN 47905	1
DIRECTOR US ARMY BALLISTIC RESEARCH LABORATORY ATTN: SLCBR-IB-M (DR. BRUCE BURNS) ABERDEEN PROVING GROUND, MD 21005-5066	1		

NOTE: PLEASE NOTIFY COMMANDER, ARMAMENT RESEARCH, DEVELOPMENT, AND ENGINEERING CENTER, US ARMY AMCCOM, ATTN: BENET LABORATORIES, SMCAR-CCB-TL, WATERVLIET, NY 12189-4050, OF ANY ADDRESS CHANGES.